CONVOLUTION AND DECONVOLUTION IN THE X-RAY DIFFRACTION ANALYSIS

David Rafaja

Faculty of Mathematics and Physics, Charles University, Ke Karlovu 5, 121 16 Prague

E-mail: rafaja@karlov.mff.cuni.cz

Abstract

A comparison of three deconvolution procedures is presented. The first technique is based on modified Stokes method. The second technique decomposes measured data into a Fourier series of harmonic functions. The third procedure regards the measured data as a linear combination of instrumental functions. It was found that the critical phenomenon influencing the quality of result is the amount of smoothing, which is contained in the respective deconvolution technique. Nevertheless, different deconvolution routines had different ranging depending on the criterion chosen. The modified Stokes method offers the shortest computing time, but it needs a higher amount of smoothing to remove noise from the experimental data. The decomposition of experimental data into a Fourier series is advantageous for use with noisy data but it is awkward for steep edges of the deconvoluted function. The linear combination of instrumental functions yields typically the best match between the experimental and the re-convoluted data, but it is time consuming.

1. Introduction

X-ray diffraction is applied to obtain information about crystalline matter on the atomic scale. The typical investigated parameters are the size and symmetry of elementary cell, positions of individual atoms within the elementary cell and atomic vibrations, see e.g. [1]. A particular method related to the X-ray diffraction, which is called diffraction profile analysis, is employed to analyse mesoscopic structure of crystalline materials. The mesoscopic structure is usually described in terms of grain size in polycrystalline materials, mechanical interaction between grains and the gradient of chemical composition and gradient of certain physical characteristics.

In the diffraction profile analysis, the decomposition of diffraction profiles is a typical task. The main problem is to separate the instrumental function (the instrumental broadening) from the measured diffraction pattern in order to obtain the pure physical profile containing information on the microstructure of materials. This means that the well-known equation for convolution

$$h(x) = f * g = \int_{-\infty}^{\infty} f(y)g(x-y)dy \tag{1}$$

must be solved for $f(y)$, which represents the wanted physical function. Function $h(x)$ describes the measured diffraction profile; $g(x\text{-}y)$ is the instrumental function (response of the apparatus). The instrumental function covers usually the line broadening due to the spectral purity of radiation, resolution of the diffractometer optics as well as a variety of instrumental aberrations. The instrumental function is either measured as the response of the apparatus or calculated taking into account all instrumental effects. As the calculation of a true instrumental function is difficult in many cases, the first approach (measurement of the instrumental function) is preferentially applied. Upon the measurement of the instrumental function, a well-known property of the convolution integral is used – convolution of a function with the Dirac distribution does not change the shape of the original function:

$$h = \delta * g = g \tag{2}$$

Such experimental data describe directly the instrumental function. The main difficulty is to find a sample, which physical function approaches the Dirac distribution with sufficient accuracy.

If the instrumental function is known, there are two different approaches how to treat the experimental data affected by instrumental broadening: direct deconvolution and indirect convolution. The latter means fitting of parameters of an appropriate model describing the physical function. The procedures based on convolutions are very popular in the last time, because they easily overcome the crucial problems arising at deconvolution. The common problems are the presence of noise in measured data and the truncation of the interval in the convolution integral (1). However, there are still numerous applications, for which the use of a deconvolution technique is inevitable [2].

A comprehensive overview of deconvolution methods was published by Čerňanský [3]. Among the large number of deconvolution methods discussed in this book, the most popular methods work with the least-square fitting of re-convoluted profiles to the measured intensities, see Ref. [4] and the references therein. The least-square method is suitable to solve integral equations of the first kind, which is also the case of the equation for convolution (1). In this paper, three procedures used for deconvolution of diffraction data are compared. The Stokes method [5] working with smoothed experimental and instrumental data, the decomposition of measured data into a Fourier series of harmonic functions [4] and the decomposition of experimental data into a linear combination of instrumental profiles.

2. Stokes method with Gaussian smoothing

2.1. Mathematical background

The classical Stokes method [5] utilises another well-known property of the Fourier transformation – the Fourier transformation of convolution of two functions can be expressed as multiplication of Fourier transforms of these functions:

$$FT(h) = FT(f * g) = FT(f) \cdot FT(g) \tag{3}$$

Consequently, the pure physical function *f* can be obtained from the measured profile *h* and from the instrumental profile *g* using the formula:

$$f = FT^{-1}\left(\frac{FT(h)}{FT(g)}\right) \equiv FT^{-1}\left(\frac{H}{G}\right) \tag{4}$$

The symbols *FT* and FT^{-1} denote the Fourier and the inverse Fourier transformation. The capitals *F*, *G* and *H* denote the Fourier transforms of functions *f*, *g* and *h*. Due to the ill-posed nature of deconvolution, which is caused mainly by the truncation of the measured interval and by the presence of noise in both the experimental and instrumental data, the formula (4) does not yield useful results. The solution is oscillating as a rule; the amplitude of the oscillations being comparable with the maximum of the deconvoluted function.

In order to overcome problems with truncation of measured intervals, the experimental data must be pre-processed. In the first step, the background is subtracted and the missing marginal data are filled by zeros. To avoid problems with the noise, the input data are smoothed. This means that typically the high-frequency noise is removed. Such a filtering of input data was used in the modified Stokes procedure presented in this contribution. Fourier transforms of both experimental and instrumental profiles were multiplied by Gaussian functions:

$$F' = \left[H \exp\left(-\frac{t^2}{\sigma_h^2}\right)\right] \Big/ \left[G \exp\left(-\frac{t^2}{\sigma_g^2}\right)\right] \tag{5}$$

This corresponds to the following combination of the Fourier transforms:

$$F' = FT(f') = \frac{FT(h)\cdot FT(s_h)}{FT(g)\cdot FT(s_g)} = \frac{FT(h * s_h)}{FT(g * s_g)} \tag{6}$$

The functions s_h and s_g are the inverse Fourier transforms of the Gaussian functions multiplying the functions *H* and *G* in Eq. (5). Further, it holds as a consequence of Eq. (6):

$$FT(h * s_h) = FT(f')\cdot FT(g * s_g) = FT(f' * g * s_g) \tag{7}$$

Applying inverse Fourier transformation on Eq. (7), we will get a similar equation for convolutions:

$$f' * g * s_g = h * s_h \equiv h * s_f * s_g \tag{8}$$

The right hand of Eq. (8) was rewritten to arrive at formally same convolutions on the left and right side. The left and right hands of Eq. (8) are equal if

$$f' = f * s_f \tag{9}$$

Equation (9) specifies the amount of smoothing in the deconvoluted profile. It can simply be shown that the deconvoluted profile is smoothed by the Gaussian function if both *g* and *h* are smoothed by Gaussian functions.

$$\begin{aligned} s_h = s_f * s_g &= FT^{-1}\left[FT(s_f)\cdot FT(s_g)\right] = FT^{-1}\left[\exp\left(-\frac{t^2}{\sigma_f^2}\right)\cdot\exp\left(-\frac{t^2}{\sigma_g^2}\right)\right] = \\ &= FT^{-1}\left[\exp\left(-t^2\cdot\frac{\sigma_f^2+\sigma_g^2}{\sigma_f^2\sigma_g^2}\right)\right] = FT^{-1}\left[\exp\left(-\frac{t^2}{\sigma_h^2}\right)\right] \end{aligned} \tag{10}$$

Therefore, the smoothing parameter σ_f is given by reciprocal difference of the parameters σ_h and σ_g:

$$\sigma_f^2 = \frac{\sigma_g^2\sigma_h^2}{\sigma_g^2 - \sigma_h^2} \tag{11}$$

The smoothing parameter σ_f describes the filtering of the Fourier transform of the deconvoluted profile:

$$FT(f') = F' = F\exp\left(-\frac{t^2}{\sigma_f^2}\right) \tag{12}$$

To derive the exact form of the smoothing function for the physical function *f*, we must perform the inverse Fourier transformation of Eq. (12):

$$f' = f * FT^{-1}\left[\exp\left(-\frac{t^2}{\sigma_f^2}\right)\right] = f * s_f, \tag{13}$$

where

$$s_f = FT^{-1}\left[\exp\left(-\frac{t^2}{\sigma_f^2}\right)\right] = \frac{1}{2\pi}\int_{-\infty}^{\infty}\exp\left(-\frac{t^2}{\sigma_f^2}\right)\cdot e^{itx}dt = \frac{1}{2\sqrt{\pi}}\sigma_f\exp\left(-\frac{x^2\sigma_f^2}{4}\right) \tag{14}$$

It follows from Eq. (14) that the smoothing function is Gaussian in form. The area below the function s_f is equal to unity,

$$\int_{-\infty}^{\infty} s_f \, dx = \frac{\sigma_f}{2\sqrt{\pi}} \int_{-\infty}^{\infty} \exp\left(-\frac{x^2 \sigma_f^2}{4} \right) dx = 1, \tag{15}$$

if the inverse Fourier transformation is defined by the formula:

$$FT^{-1}(F) = \frac{1}{2\pi} \int_{-\infty}^{\infty} F(t) e^{itx} dt \tag{16}$$

In such a case, the smoothing has no effect on the integral of the deconvoluted function.

Equation (11) has several important consequences. The deconvoluted profile is automatically smoothed if the experimental data and the instrumental profile are smoothed. For correct smoothing, σ_h must be less than σ_g, which means that the experimental function *h* must be filtered to lower frequencies than the instrumental function *g*. If σ_h and σ_g have approximately the same value, σ_f is very high. Thus, the physical function *f* is not smoothed at all. If σ_g is much larger than σ_h, the smoothing of *f* is extreme – it is the same as the smoothing of *h*.

2.2. Results

Substantial part of the computer code for deconvolution routine based on the modified Stokes is shown in Fig. 1. Fourier transforms were calculated using the internal MATLAB® function for the fast Fourier transformation and the inverse Fourier transformation. Variables `hy` and `gy` contain the experimental data and the instrumental function, respectively. The quality of the deconvoluted data was measured by the agreement between the original experimental data $h(x)$ and the re-convoluted function $h_r(x)$:

$$\chi = \sqrt{\frac{\sum_{i=1}^{n} [h_r(x_i) - h(x_i)]^2}{n(n-1)}} \tag{17}$$

The re-convoluted function was obtained by convoluting the deconvoluted function with the instrumental function:

$$h_r = f * g \tag{18}$$

For the back convolution, the standard routine shown in Fig. 2 was used. The experimental data, the instrumental function, the deconvoluted data, the re-convoluted function and the difference between the experimental and the re-convoluted data are shown in Fig. 3. For the modified Stokes method with Gaussian smoothing, the sum of residuals was 6.3 %. The largest differences were found at the rising edge of the experimental function and at the maxima.

3. Decomposition of experimental functions using Fourier expansion

3.1. Mathematical background

The second procedure presented here is decomposition of the measured data, which uses expansion of the physical function into the Fourier series. This approach is especially advantageous if subsequent method of data reduction works with the Fourier coefficients, which are directly obtained upon this

calculation. The computing routine is completely based on the technique, published by Sánchez-Bajo and Cumbrera in [4]. The only exception is that we took the instrumental profile in its measured form, instead of approximating it by an expansion into the Hermite polynomials like in [4]. Employing the expansion of the physical function into a Fourier series, function *f* takes the form:

$$f(x)=\sum_{j=0}^{m} C_j \cos(j\omega_0 x)+\sum_{j=1}^{m} S_j \sin(j\omega_0 x) \quad \text{with} \quad \omega_0=\frac{2\pi}{\Delta} \tag{19}$$

The symbol Δ in Eq. (19) defines the width of the interval, in which the experimental data were measured. Regarding the equation for convolution (1), the experimental function can be written as:

$$\begin{aligned} h(x)&=\int_{-\infty}^{\infty} g(x-y)\cdot\left[\sum_{j=0}^{m} C_j \cos(j\omega_0 y)+\sum_{j=1}^{m} S_j \sin(j\omega_0 y)\right]dy= \\ &=\sum_{j=0}^{m} C_j \int_{-\infty}^{\infty} g(x-y)\cos(j\omega_0 y)dy+\sum_{j=1}^{m} S_j \int_{-\infty}^{\infty} g(x-y)\sin(j\omega_0 y)dy \end{aligned} \tag{20}$$

Equation (20) represents convolutions of the instrumental function *g* with the basis of harmonic functions:

$$h(x)=\sum_{j=0}^{m} C_j [g*\cos(j\omega_0 y)]+\sum_{j=1}^{m} S_j [g*\sin(j\omega_0 y)] \tag{21}$$

Within the implementation of the deconvolution procedure, Eq. (21) is solved for the Fourier coefficients C_j and S_j in the least-square sense. This means that the sum of residuals, χ^2, is minimised:

$$\chi^2=\sum_{i=1}^{n}\left(\frac{\sum_{j=0}^{2m} b_j\varphi_j(x_i)-h(x_i)}{\sigma_i}\right)^2=\min \tag{22}$$

The meaning of variables in Eq. (22) is the following: *n* is the number of experimental data, σ their statistical weight and *b* the Fourier coefficients (sine and cosine). The functions φ express the convolution of the instrumental function *g* with the respective harmonic function (sine or cosine). The condition (22) is fulfilled if the derivatives of χ^2 are equal to zero:

$$\frac{\partial\chi^2}{\partial b_k}=\sum_{i=1}^{n}\left(\frac{2}{\sigma_i^2}\sum_{j=0}^{2m} b_j\varphi_j\varphi_k\right)-\sum_{i=1}^{n} 2h\varphi_k/\sigma_i^2=0\,;\ k=0,\ldots,2m \tag{23}$$

This implies the system of (2*m*+1) linear equations:

$$\sum_{i=1}^{n}\left(\sum_{j=0}^{2m} b_j\varphi_j(x_i)\varphi_k(x_i)\Big/\sigma_i^2\right)=\sum_{i=1}^{n} h(x_i)\varphi_k(x_i)/\sigma_i^2\,;\ k=0,\ldots,2m \tag{24}$$

The above system of equations can be rewritten into the matrix form:

$$\mathbf{Mb}=\mathbf{A}\text{, where } \mathbf{M}=\mathbf{\Phi}^T\mathbf{\Phi} \text{ and } \mathbf{A}=\mathbf{h}^T\mathbf{\Phi} \tag{25}$$

The matrix **Φ** and the vector **h** have the form:

$$\mathbf{\Phi} = \begin{pmatrix} \varphi_0(x_1)/\sigma(x_1) & \varphi_1(x_1)/\sigma(x_1) & \varphi_2(x_1)/\sigma(x_1) & \cdots \\ \varphi_0(x_2)/\sigma(x_2) & \varphi_1(x_2)/\sigma(x_2) & \varphi_2(x_2)/\sigma(x_2) & \cdots \\ \varphi_0(x_3)/\sigma(x_3) & \varphi_1(x_3)/\sigma(x_3) & \varphi_2(x_3)/\sigma(x_3) & \cdots \end{pmatrix}; \ \mathbf{h} = \begin{pmatrix} h(x_1) \\ h(x_2) \\ h(x_3) \\ \vdots \end{pmatrix} \tag{26}$$

The wanted Fourier coefficients are the solution of Eq. (25):

$$\mathbf{b} = \mathbf{M}^{-1}\mathbf{A} \tag{27}$$

Application of this deconvolution routine implies an automatic smoothing of deconvoluted data. The amount of smoothing is determined by a number of harmonic functions (variable *m* in Eq. (19)-(24)). The lower *m*, the higher is the degree of smoothing.

3.2. Results

The convolutions in Eq. (21) were calculated with the aid of the fast Fourier transformation and the inverse fast Fourier transformation (see Eq. (3)). The related computer code is illustrated in Fig. 2. The least-square refinement of the coefficients C_j and S_j is performed successively for increasing number of harmonic functions, *m* (see the part of the computer code in Fig. 4). Because of large expected asymmetry of deconvoluted functions, harmonic functions up to the 40th order were tested. The best set of C_j and S_j was selected according to the lowest sum of residuals between the original data *h* and the re-convoluted data h_r (Eq. (17)) obtained from the back convolution (18). The deconvoluted function is calculated using Eq. (19). The result of the deconvolution using the Fourier expansion is shown in Fig. 5 in graphical form. The sum of residuals is steeply decreasing with the order of harmonic functions reaching approximately 7 % at *m* = 19 in this case (see Inset in Fig. 5). In comparison with the modified Stokes method, the decomposition of experimental data using the Fourier expansion offers much higher degree of smoothing. The degree of smoothing is inversely proportional to the number of the harmonic functions used for the calculation. However, the modified Stokes method is much faster.

4. Experimental profile regarded as linear combination of instrumental profiles

4.1. Mathematical background

The last deconvolution procedure solves the equation for convolution (1) in the form used for discrete data:

$$h_m = \sum_{n=-\infty}^{\infty} f_n g_{m-n} \tag{28}$$

In matrix representation, Eq. (28) takes the form:

$$\begin{pmatrix} g_0 & g_{-1} & g_{-2} & g_{-3} & \cdots \\ g_1 & g_0 & g_{-1} & g_{-2} & \cdots \\ g_2 & g_1 & g_0 & g_{-1} & \cdots \\ g_3 & g_2 & g_1 & g_0 & \cdots \\ \vdots & \vdots & \vdots & \vdots & \ddots \end{pmatrix} \cdot \begin{pmatrix} f_1 \\ f_2 \\ f_3 \\ f_4 \\ \vdots \end{pmatrix} = \begin{pmatrix} h_1 \\ h_2 \\ h_3 \\ h_4 \\ \vdots \end{pmatrix} \tag{29}$$

The meaning of the matrices **G** and **H** can be illustrated on two limit cases. The Dirac δ-function corresponds to an identity matrix for the instrumental function or to a single "one" embedded in a zero matrix for the deconvoluted function. The crucial problem of the solution is that Eq. (29) represents an infinite system of linear equations. Moreover, the system of equations is in fact underestimated, as the data contain noise (random errors). Therefore, some assumptions must be done to reduce the number of unknown parameters in the linear combination (28).

In contrast to the deconvolution procedures employing the Fourier transformation, we can assume here that the deconvoluted intensities are equal to zero outside a certain range. This assumption reduces substantially the number of columns in the **G** matrix (Eq. (29)). It means that the system of linear equations becomes overestimated. Thus, it can be solved using the least-square method. However, it is still necessary to filter the noise in deconvoluted data. For filtering, the Fourier smoothing or the Golay-Savitzky method [6] were alternatively applied. The Fourier smoothing means a convolution of the deconvoluted profile with a Gaussian function like in the modified Stokes method (see, Eq. (5)). The Golay-Savitzky method represents a "per partes" approximation of the original function by a polynomial without Fourier transformations.

4.2. Results

Regarding the match between the experimental and re-convoluted data, this method yields the best results. However, it has two disadvantages. First, the size of the matrices in Eq. (29) and thus the computing time are increasing with the number of experimental data. Time consuming are both the composition of the kernel and the solution of overestimated system of linear equations (Fig. 6). Secondly, as this procedure does not include automatic smoothing, the deconvoluted intensities contain typically a high amount of noise. Therefore, additional smoothing is needed. The "as received" and smoothed deconvoluted patterns are shown in Fig. 7. The smoothing in the bottom pattern is the same as for the modified Stokes method. Before smoothing, the sum of residuals was approximately 2 %, after smoothing it reached nearly 5 %.

5. Comparison of the deconvolution methods

It can be seen from Figures 3, 5 and 7 that the deconvolution methods presented here yield similar results. Nevertheless, some differences can be found, which are caused mainly by different amount of smoothing included in the respective technique. Consequently, the critical cases for deconvolution are the similar shapes of the experimental and instrumental functions or the steep edges of the physical (deconvoluted) function. Two examples are given in Figures 8 and 9. The first one (Fig. 8) shows deconvolution of the same functions, which should result in the Dirac distribution (see Eq. (2)). Only the results of the modified Stokes method and linear combination of instrumental functions are compared, because the decomposition of experimental data into a Fourier series did not yield a convergent solution within a reasonable order of harmonic functions. This example illustrates also the influence of smoothing on the quality of the re-convoluted function. Typically, maxima of the re-convoluted function decrease and broaden after smoothing, which is the consequence of additional convolution of the deconvoluted function with a smoothing function (Section 2.1). The second example compares results of all three deconvolution methods applied to a function with steep rising edge. The dominant differences between the original and the re-convoluted data are again at the sharp maximum (see Fig. 9).

6. Conclusions

Three deconvolution routines were compared: the Stokes method with Gaussian smoothing, the decomposition of experimental data into a Fourier series and the decomposition of experimental data into a linear combination of instrumental functions. The deconvoluted functions differ substantially only in extreme cases, if a high degree of smoothing is unfavourable. This is the case, for instance, if

the deconvoluted function is very narrow, or if one of the edges of the physical function is very steep. The advantages and disadvantages of the deconvolution routines can be summarised as follows. The modified Stokes method offers the shortest computing time but it needs a higher degree of smoothing to obtain a non-oscillating solution. The decomposition of experimental data into a Fourier series offers the best smoothing. Therefore, it is not favourable to be applied on functions with sharp edges. Finally, the decomposition of experimental functions into a linear combination of instrumental functions offers the best match between the original and re-convoluted data but it is most time consuming.

References

[1] C. Giacovazzo, H.L. Monaco, D. Viterbo, F. Scordari, G. Gilli, G. Zanotti and M. Catti: Fundamentals of Crystallography, International Union of Crystallography, Oxford University Press, New York, 1994.

[2] D. Rafaja, Materials Structure, in press.

[3] M. Čerňanský: Restoration and pre-processing of physical profiles from measured data *in* R.L. Snyder, J. Fiala and H.J. Bunge (ed.), Defect and Microstructure Analysis by Diffraction, International Union of Crystallography, Oxford University Press, 1999.

[4] F. Sánchez-Bajo and F.L. Cumbrera, J. Appl. Cryst. 33 (2000) 259.

[5] A.R. Stokes, Proc. Phys. Soc. 61 (1948) 382.

[6] A. Savitzky and M.J.E. Golay, Anal. Chem. 36 (1964) 1627.

Figures:

Figure 1: A part of the implementation of the Stokes method with Gaussian smoothing. Functions `hy`, `gy` and `fy` mean the measured data, the instrumental function and the deconvoluted function, respectively.

```
% Fourier transforms of hy and gy
HH = fft([hy zeros(1,length(gy)-1)]);
GG = fft([gy zeros(1,length(hy)-1)]);
% Smoothing of HH
sigma = length(HH)/20; x = 1:length(HH);
gauss = exp(-(x.^2)/sigma^2);
gauss = gauss + fliplr(gauss);
HH = gauss.*HH;
% Smoothing of GG
sigma = length(GG)/5; x = 1:length(GG);
gauss = exp(-(x.^2)/sigma^2);
gauss = gauss + fliplr(gauss);
GG = gauss.*GG;
ft = real(ifft(HH./GG)); ft = fftshift(ft);
```

Figure 2: The computer code for convolution used to check the quality of deconvoluted data. The meaning of variables is the same as in Fig. 1.

```
% Back convolution
FF = fft([fy zeros(1,length(gy)-1)]);
GG = fft([gy zeros(1,length(fy)-1)]);
ht = real(ifft(FF.*GG));
```

Figure 3: Result of the modified Stokes method. The measured data are plotted by thick solid line, the deconvoluted data by the thin line. The differences between the measured and re-convoluted data [`diff = 2*(h-hr)-10`] are at the bottom. The shape of the instrumental function is shown in the Inset.

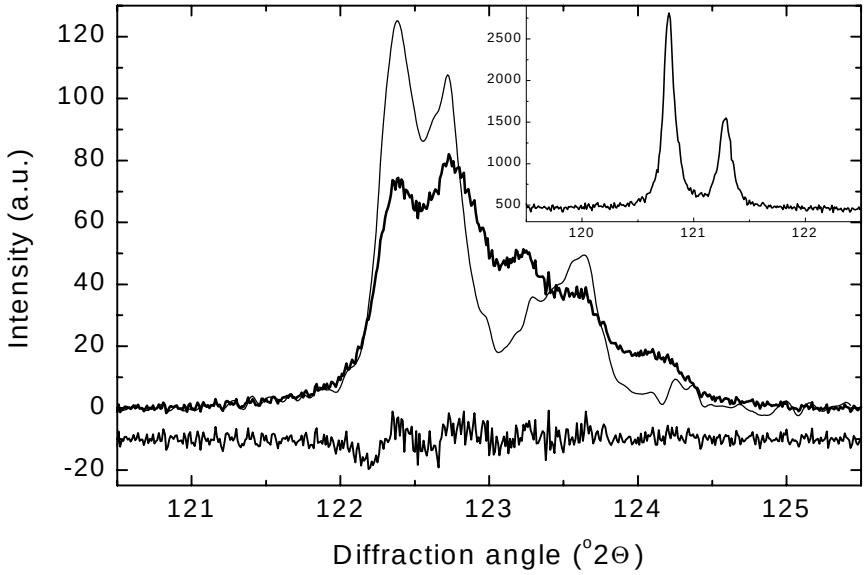

Figure 4: A part of the computer code used for decomposition of experimental data into a Fourier series. The variable `hx` contains the *x* values for the experimental function `hy`; `gy` is the instrumental function. The integer `jjj` denotes the maximum order of the harmonic functions in the Fourier series.

```
omega = 2*pi/(hx(end)-hx(1));
for jj = 1:jjj,
   fc(jj,:) = cos(jj*omega*hx);
   fs(jj,:) = sin(jj*omega*hx);
   FF = fft([fc(jj,:) zeros(1,length(gy)-1)]);
   GG = fft([gy zeros(1,length(fc(jj,:))-1)]);
   phic(:,jj) = (real(ifft(FF.*GG)))'./sigma;
   FF = fft([fs(jj,:) zeros(1,length(gy)-1)]);
   phis(:,jj) = (real(ifft(FF.*GG)))'./sigma;
end

for jj = 1:jjj,
   HH = [hy zeros(1,length(gy)-1)];
   phi = [ones(length(HH),1)./sigma phic(:,1:jj) phis(:,1:jj)];
   M  = phi' * phi;
   A  = (HH./sigma' * phi)';
   b  = inv(M)*A;
   fy = ones(1,length(hy))*P(1)/sum(gy);
   fy = fy + (P(2:(jj+1)))'*fc(1:jj,:);
   fy = fy + (P((jj+2):(2*jj+1)))'*fs(1:jj,:);
end
```

Figure 5: Result of the decomposition of measured data into the Fourier series of 19 harmonic functions. The measured data are plotted by the thick line, the deconvoluted data by the thin line. The differences between the measured and re-convoluted data [`diff = 2*(h-hr)-10`] are at the bottom. The sum of residuals is shown in the Inset; it is plotted as a function of the number of harmonic functions.

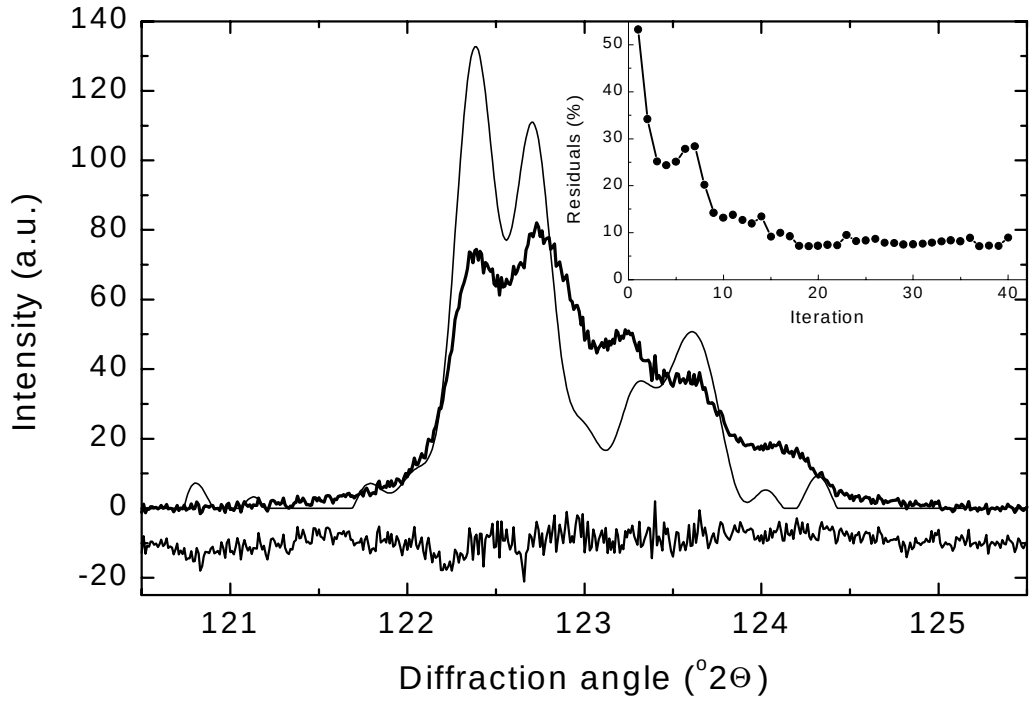

Figure 6: Computer code used for composition of the kernel and for solving the overestimated system of linear equations in the decomposition of experimental data into a linear combination of instrumental functions.

```
% Compose the kernel
lh = length(h);
for ii = 1:lh ,
  GG(ii,:) = g((g0-ii+1):(g0-ii+lf));
end

% Solving the system of linear equations
fy = (GG\HH)'*sum(gy);
```

Figure 7: Results of the decomposition of measured data into the linear combination of instrumental functions. At the top, deconvoluted and re-convoluted data are shown as received from the deconvolution procedure without smoothing. The figure at the bottom shows the deconvoluted and re-convoluted data after smoothing corresponding to that used for the modified Stoked method. Measured data are plotted by thick lines, deconvoluted data by thin lines. Differences between the measured and re-convoluted data [`diff = 2*(h-hr)-10`] are plotted below the measured data in the respective figure.

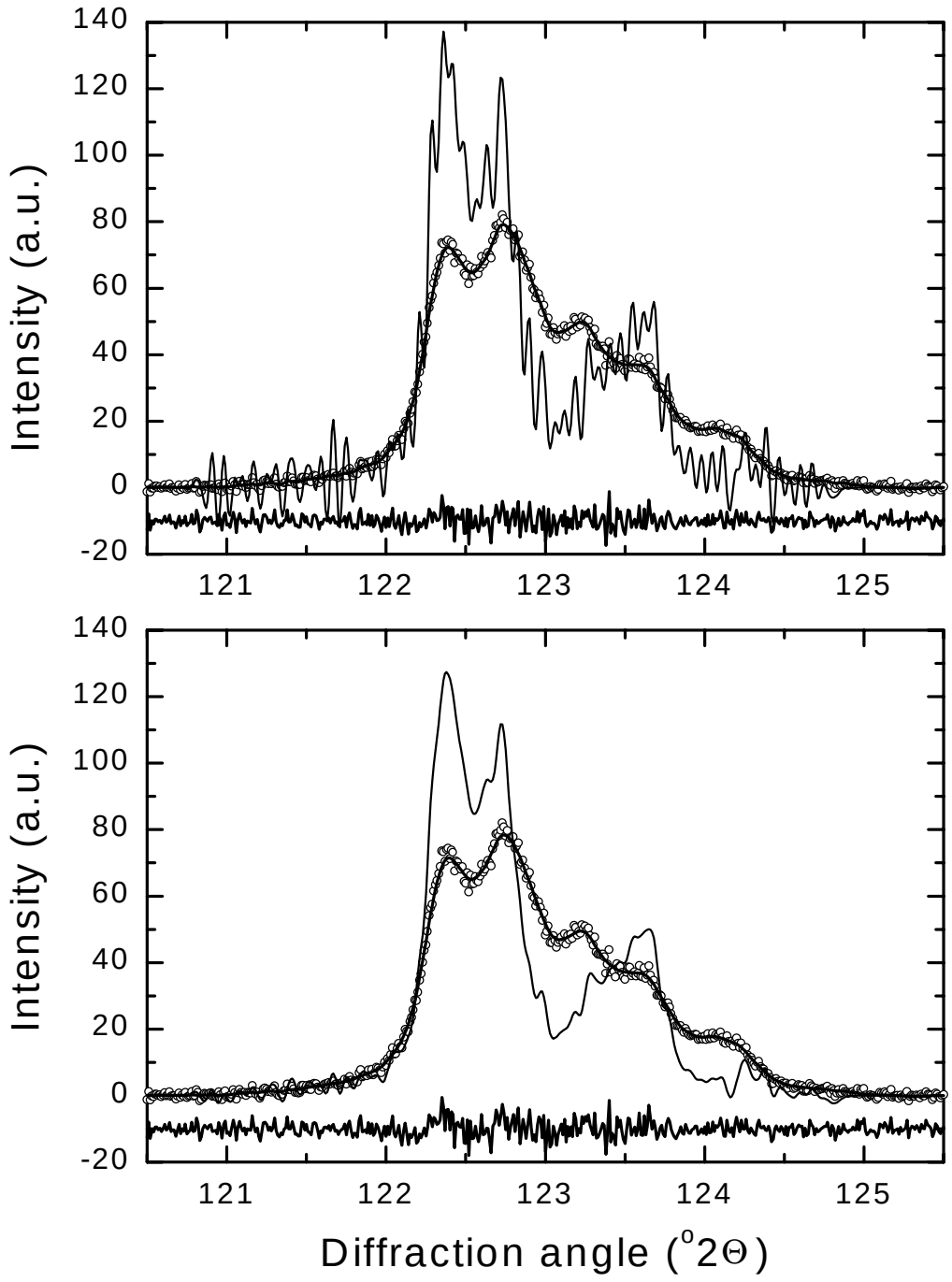

Figure 8: Comparison of deconvoluted data obtained from the modified Stokes method (a) and from the linear combination of instrumental functions (b). The instrumental function had the same shape as the experimental data. Measured data are represented by open circles, the re-convoluted data by solid lines. Deconvoluted intensities are shown in the bottom figure. The Inset shows poor reconstruction of the re-convoluted data due to the smoothing.

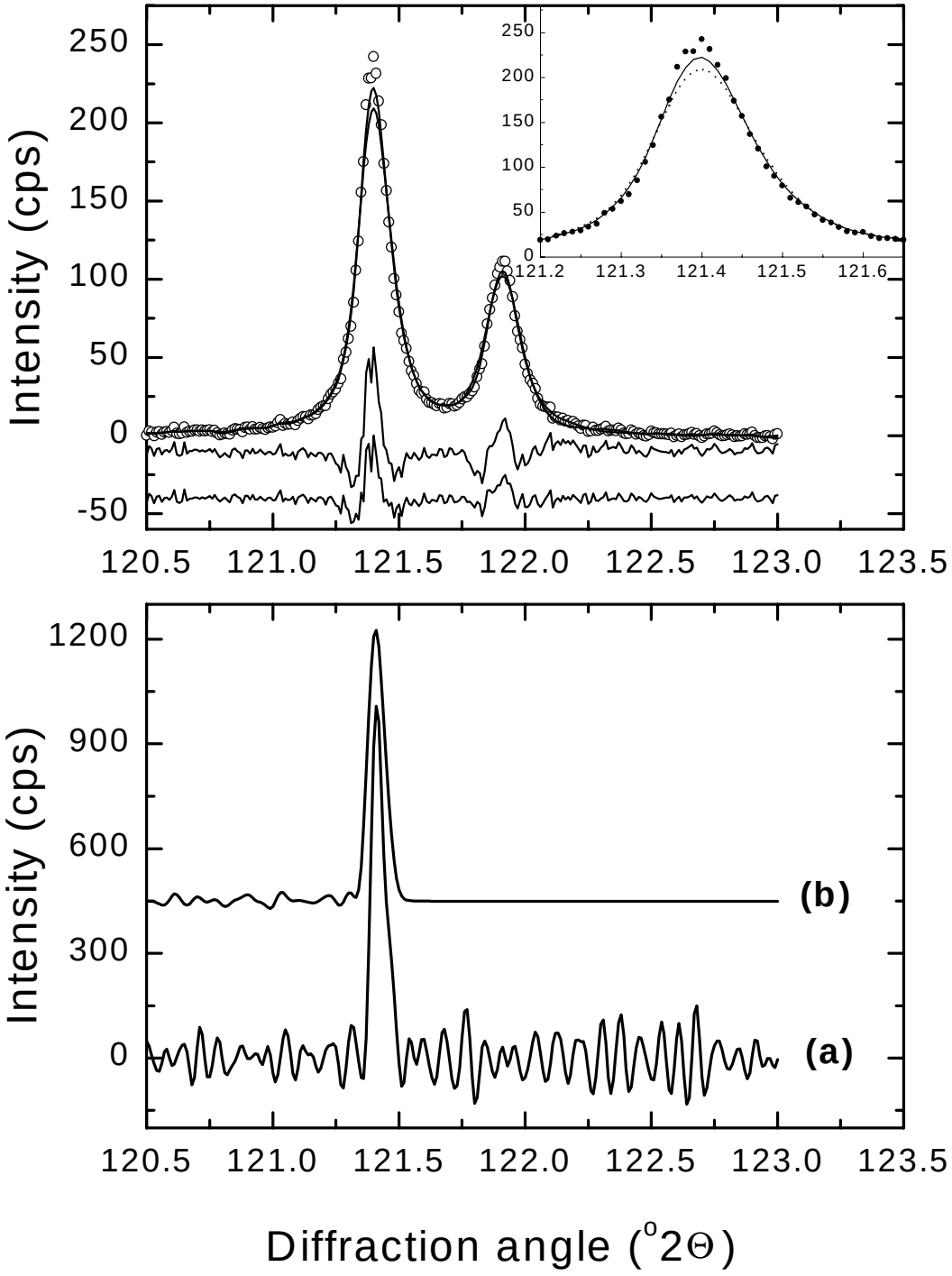

Figure 9: Results of the deconvolution procedures applied to the function with a steep edge. Figure at the top: experimental data are plotted by thick solid line; the differences between the original and the re-convoluted data are shifted down. Figure at the bottom: deconvoluted functions as obtained from the modified Stokes method (thick line), expansion to Fourier series (thin line) and linear combination of instrumental functions (interconnected dots). The same symbols are also used for the differences above.